BIOCHEMISTRY
including biophysical chemistry & molecular biology

ARTICLE

pubs.acs.org/biochemistry

Mapping the Protein−Protein Interface between a Toxin and Its Cognate Antitoxin from the Bacterial Pathogen *Streptococcus pyogenes*

Justin B. Sperry,[†,‡] Craig L. Smith,[§] Michael G. Caparon,[⊥] Tom Ellenberger,[§] and Michael L. Gross*[,‡]

[†]Analytical Research and Development, Pfizer Inc., Chesterfield, Missouri 63017, United States

[‡]Department of Chemistry, Washington University in St. Louis, St. Louis, Missouri 63130, United States

[§]Department of Biochemistry and Molecular Biophysics and [⊥]Department of Molecular Microbiology, Washington University in St. Louis, St. Louis, Missouri 63110, United States

Supporting Information

ABSTRACT: Protein−protein interactions are ubiquitous and essential for most biological processes. Although new proteomic technologies have generated large catalogs of interacting proteins, considerably less is known about these interactions at the molecular level, information that would aid in predicting protein interactions, designing therapeutics to alter these interactions, and understanding the effects of disease-producing mutations. Here we describe mapping the interacting surfaces of the bacterial toxin SPN (*Streptococcus pyogenes* NAD^+ hydrolase) in complex with its antitoxin IFS (immunity factor for SPN) by using hydrogen−deuterium amide exchange and electrospray ionization mass spectrometry. This approach affords data in a relatively short time for small amounts of protein, typically 5−7 pmol per analysis. The results show a good correspondence with a recently determined crystal structure of the IFS−SPN complex but additionally provide strong evidence for a folding transition of the IFS protein that accompanies its binding to SPN. The outcome shows that mass-based chemical footprinting of protein interaction surfaces can provide information about protein dynamics that is not easily obtained by other methods and can potentially be applied to large, multiprotein complexes that are out of range for most solution-based methods of biophysical analysis.

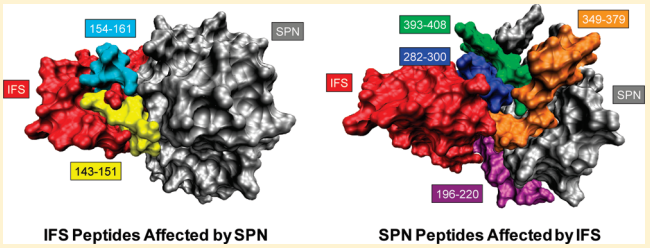

Nearly all biological functions involve the interaction of one protein with another; for example, many cellular tasks are achieved by the coordinated action of a dimeric or multimeric protein assembly.[1] The formation of these protein assemblies affords some of the most complex architectures in biology; the specificity of these interactions has become one of the most studied problems in the biological sciences.[2−5] Protein interactions require specific recognition between partners to form the interface.[6−9] Interfaces can be categorized into two subclasses: homomeric and heteromeric. Heteromeric interfaces are those pertaining to two or more different polypeptide chains that form noncovalent higher order structures. Each protein is synthesized separately by the cell, and the complex forms under appropriate biological conditions.[6] Formation of each of these interfaces is thermodynamically driven[10,11] and usually the result of many factors including hydrophobic effects,[12−14] interaction of electrostatically charged polar residues,[15−17] and formation of new hydrogen bonds.[18−20]

There are many techniques used for the structural characterization of protein−protein interfaces; they include cryo-electron microscopy (cryo-EM),[21] nuclear magnetic resonance (NMR),[22−25] infrared microscopy (IR),[26] the yeast two-hybrid assay (Y2H),[27,28] fluorescence resonance energy transfer (FRET),[29,30] and, most commonly, X-ray crystallography.[31−34] X-ray crystallography, however, requires the multimeric protein complex to be produced at high concentrations and be amenable to crystal formation. These methods involve trade-offs in resolution, protein-sample requirements, experimental effort, and inability to capture the dynamics of the interacting proteins. Mass spectrometry (MS) is a flexible platform for protein analysis; it can accommodate a variety of approaches to identify interacting proteins and to characterize their interactions.[35,36] Some of these approaches use affinity tags,[37] hydrogen−deuterium amide exchange,[38,39] chemical footprinting,[40,41] and chemical cross-linking.[42] The utility and interest of hydrogen−deuterium exchange to characterize protein−protein interfaces are increasing, as demonstrated in several recent examples.[43−49] Mass spectrometry-based approaches do suffer, however, drawbacks related to protein-sequence coverage. Region-specific structural information on proteins is highly dependent on the ionization properties of peptides resulting from digestion. Taking these into consideration, we wish to apply a mass spectrometric approach to aid in the determination of a protein−protein interface.

Protein−protein interactions are important for bacterial pathogens[50,51] including *Streptococcus pyogenes*[52,53] (*S. pyogenes*) or, more generally, group A strep. To enhance infectivity, *S. pyogenes* injects the

Received: February 17, 2011
Revised: April 1, 2011
Published: April 05, 2011

SPN NAD^+-glycohydrolase into host cells,[54−56] catalyzing the destruction of β-$NAD^+$and altering host-cell metabolism.[57−61] SPN is also toxic to *S. pyogenes*. SPN-producing strains, however, are protected by expressing in its cytoplasm a specific antitoxin named IFS (immunity factor for SPN)[57] or SNI (streptococcal NADase inhibitor)[62] that binds to SPN as a competitive inhibitor with respect to the β-NAD^+ substrate.[63−65] IFS−SPN forms a stable protein complex that was recently crystallized, revealing how bound IFS forms a lid over the SPN active site.[66] Understanding these interactions should have implications for developing therapeutics against *S. pyogenes*.

We report here the use of a region-specific H/D exchange (H/DX) protocol to probe the binding interface of the IFS−SPN complex, first analyzing each protein separately followed by determining changes in H/DX upon complex formation. Regions of the protein that show decreased exchange upon complex formation must either be buried in the protein−protein interface or become restructured upon binding to a partner protein. Using H/DX methods, we show that the native fold of IFS changes in conjunction with binding to SPN. A similar coupling of protein folding and binding is recognized to contribute to the specificity of a growing number of protein−protein interactions.[67,68]

EXPERIMENTAL SECTION

Materials. Deuterium oxide, sodium chloride, formic acid, calcium chloride, acetonitrile, and Tris buffer were purchased from Sigma-Aldrich (St. Louis, MO) at the highest purity available. Immobilized pepsin on agarose was purchased from Pierce (Rockford, IL). IFS and SPN proteins were prepared in the Ellenberger laboratory using previously published techniques and used without further purification.[66] The molecular mass of IFS was determined to be 21 960 ± 1 Da by electrospray ionization mass spectrometry (ESI-MS); the protein included a small linker (FRSF), a C-terminal c-myc tag (residues 170−181), a second small linker (NSAV), and a His tag (residues 182−187). The base peak in the SPN ESI mass spectrum corresponded to an N-terminal truncation between residues 36 and 37, and the molecular mass was determined to be 46 026 ± 1 Da.

H/D Exchange Kinetics. Protein stock solutions (30 μM for IFS and 40 μM for SPN) were prepared in 20 mM Tris (pH = 8.8) and 50 mM NaCl. H/D exchange kinetics experiments were conducted with three samples: IFS alone, SPN alone, and IFS−SPN complex (1:1 molar ratio). To initiate exchange, 0.5 μL of the protein stock was diluted with 20 μL of D_2O containing 20 mM Tris and 50 mM NaCl at 25 °C to give a D_2O content of >97%. At various times the exchange was quenched with ice cold 1.0 M HCl to give a final pH of 2.0. The K_I of IFS to SPN was determined to be on the order of 2 nM;[57] therefore, the complex should be nearly 100% bound at low micromolar concentrations during the H/D exchange studies.

To determine deuterium uptake at the peptide level, 5 μL of immobilized pepsin on agarose was added to the quenched solution to release various peptides from the protein. The digestion took place for 3 min at 0 °C with a quick vortexing pulse every 15 s. After digestion, the beads were briefly centrifuged (2−3 s) so that they settled at the bottom of the sample tube. The supernatant solution containing the digested protein was loaded on a C_{18} column (LC Packings, 1 × 15 mm, PepMap cartridge, Dionex Corp., Sunnyvale, CA) that was pre-equilibrated with 100 μL of 0.2% formic acid in water (0 °C). The column was washed with 300 μL of 0.2% formic acid in water (0 °C), back-exchanging the labile sites of the peptides and undigested protein. The peptides were separated by HPLC with a gradient (10% B to 40% B in 9 min, 40% B to 80% B in 1 min, 80% B to 40% B in 2 min, 40% B to 10% B in 1 min, then 10% B for equilibration) at a flow rate of 40 μL/min. To minimize back-exchange, the incoming/outgoing LC solvent line, injection valve, and sample loop were submersed in ice (0 °C).

LC-ESI/MS Analysis with a Q-TOF Mass Spectrometer. All ESI mass spectra of the exchanging protein and peptides were acquired in the positive-ion mode on a Waters (Micromass) Q-TOF Ultima (Manchester, U.K.) equipped with a Z-spray ESI source. The capillary voltage was 3.2 kV, cone voltage readback of 100 V, and the source and desolvation temperatures were 80 and 180 °C. The cone and desolvation gas flows were 40 and 400 L/h. The MS profile used for quadrupole transmission was from m/z 500, dwell for 5% of the scan time, ramp to m/z 1000 for 45% of the scan time, and then dwell at m/z 1000 for 50% of the scan time.

LC-ESI/MS-MS Analysis of Protein Digest. Peptides produced by pepsin cleavage were identified by accurate mass and product-ion sequencing on a LTQ-Orbitrap hybrid mass spectrometer (Thermo, San Jose, CA). After 3 min of pepsin digestion, following the protocol above, the solution was loaded onto a C_{18} custom-packed column (75 μm i.d., 10 cm length). The peptides were separated over 80 min using an Eksigent NanoLC-1D (Dublin, CA) with an LC gradient (2% B hold for 5 min, 2% to 50% B in 60 min, 50% B to 80% B in 15 min, 80% B hold for 2 min, 80% B to 2% B in 3 min, then 2% B for equilibration) at 260 nL/min. The solution was sprayed directly from the column into the mass spectrometer by using a PicoView PV-500 nanospray source (New Objective, Woburn, MA) attached to the LTQ-Orbitrap. A full mass spectrum was recorded in the Orbitrap part of the instrument, operating at 60 000 mass resolving power at m/z 400, and data-dependent product-ion spectra of precursors identified by the Orbitrap were collected by the ion trap. The MS/MS experiments carried out in the LTQ utilized wide-band activation and dynamic exclusion. The resulting accurate mass and product-ion spectra were searched against a database by using Mascot (Matrix Science, Oxford, UK).

Data Analysis. The protein mass spectrum at each H/D exchange time point was deconvoluted by using the MaxEnt1 algorithm (MassLynx 4.0), and the deuterium level at each time point was determined by subtracting the average mass of the undeuterated protein from the average mass of the deuterated protein. The rate of back exchange was measured to be 1 deuterium loss per min. Ion signals for the deuterated peptides were smoothed twice in MassLynx with a Savitsky−Golay algorithm and imported into Microsoft Excel as an x,y pair (mass, intensity). The centroid and width of the deuterium distribution for each peptide was analyzed using HX-Express software.[69] The back-exchange occurs at the same rate as in the experiment in which the intact protein was investigated; however, no corrections were made for this back exchange because only relative (not absolute) deuterium levels were compared in all experiments. The deuterium uptake plots were fit using a pseudo-first-order kinetics model as described previously.[70] All of the experiments were conducted in triplicate, and the precision was shown as ±1 standard deviation as error bars in the H/DX uptake plots.

RESULTS AND DISCUSSION

H/D Exchange of the Full-Length Proteins. The forward H/D exchange (H/DX) experiments were conducted over a 60 min time course on three different samples: IFS alone, SPN alone, and IFS-SPN as a 1:1 complex. The deuterium uptake data for the intact protein were obtained by using the undigested protein

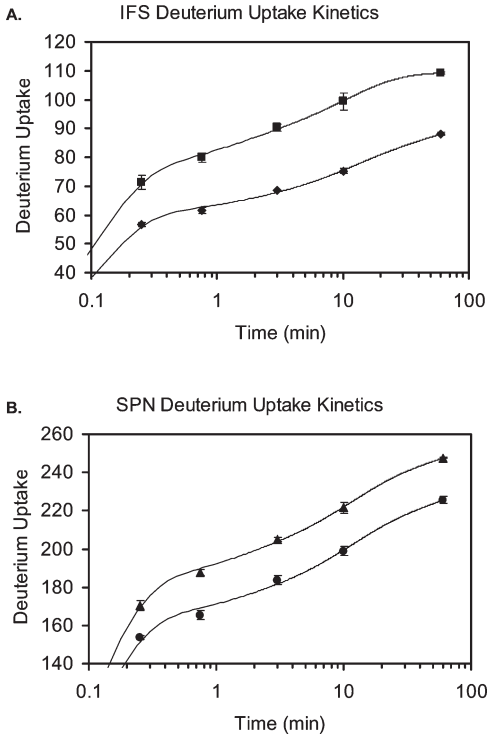

Figure 1. (A) Global H/D exchange kinetics experiment of IFS alone (squares) and IFS in the presence of SPN (diamonds). A protection change is observed in IFS upon binding SPN. (B) Global H/D exchange kinetics experiment of SPN alone (triangles) and SPN in the presence of IFS (circles). A protection change is observed in SPN upon binding IFS. H/D exchange was conducted over a 60 min time course with 97% D_2O content.

remaining in the sample after 3 min of proteolytic digestion at 0 °C. The deuterium levels in the digested products were determined at each time point (0.25, 0.75, 3, 10, and 60 min) by subtracting the average (centroid) mass of the undeuterated protein from the average mass of the deuterated protein.

A plot of deuterium uptake versus time for IFS reveals that hydrogen bonding increases upon binding SPN, affording "protection" to the protein as indicated by a decreased deuterium uptake with time (Figure 1A). After 3 min of H/DX, IFS alone shows an upward mass shift of 90 ± 1 Da, and, in the presence of SPN, a lower mass shift of 69 ± 1 Da. This result implicates 21 (90 − 69) amide hydrogens that become "protected" by binding SPN. IFS has a total of 182 exchangeable amide sites (187 amino acids minus four proline residues and the fast-exchanging N-terminus). A normalization of the deuterium uptake to the number of exchangeable amide sites on the protein indicates that the percent deuteration of IFS is 50% in the apo state and 38% in the presence of SPN. Subtracting the two numbers gives a "protection" of ∼12%. At all H/DX times, IFS is on average 10% protected upon binding SPN, indicating that the protein−protein complex is not transient. If it were transient (i.e., has a large k_{off}), then the deuterium uptake curves would come together at long times.

On the basis of the results for IFS, amides in SPN should also show protection upon binding, and indeed this is realized (Figure 1B). At 3 min of H/DX, SPN alone has a mass shift of 205 ± 1 Da, and in the presence of IFS, the mass shift is 184 ± 2 Da. This result implicates 21 amide hydrogens that are "protected" by the binding of IFS. SPN has a total of 414 exchangeable amide sites (423 amino acids, of which eight are prolines and one fast-exchanging N-terminus); hence, SPN becomes 50% deuterated when alone and 44% deuterated in the presence of IFS. The difference of ∼6% is a measure of the effect of binding IFS. The protection in SPN remains constant at all H/DX times, a result that is similar to that observed for IFS.

The "protection" shown by each protein is a result of increased H-bonding and decreased solvent accessibility at the protein−protein interface. Although SPN is roughly twice the size of IFS, similar numbers of amide hydrogens are "protected" in both proteins upon formation of the IFS−SPN complex.

Region-Specific H/D Exchange of IFS. We now describe results that localize the sites with decreased rates of H/DX that form the protein−protein interface. Digestion of the deuterated IFS alone and in the presence of SPN affords region-specific information regarding the extent of deuterium incorporation and the location of those changes upon complex formation. Several regions of IFS do not show any change in the extent of H/DX, whereas other regions show significant changes between IFS alone and in the complex with SPN. Some of the residues in the C-terminal portion of IFS are strongly protected in the IFS−SPN complex (Figure 2). We see this beginning with the peptide spanning residues 120−142. In unbound IFS, this peptide shows a significant time-dependent extent of deuteration (e.g., from 30% at 15 s to 70% at 60 min). In the presence of SPN, the percent deuteration is decreased by ∼10% at all exchange times, indicating that a few residues in this peptide are stably sequestered in complex with SPN (Figure 2).

Peptides 143−151 and 154−161 show dramatic changes upon binding SPN. For example, 143−151 becomes greater than 75% deuterated at long times, indicating that the corresponding region of the protein is solvent-exposed and/or unstructured in the absence of SPN. Upon complex formation, however, the extent of HDX decreases ∼33%. In the IFS−SPN complex, this segment comprises the SPN-interacting loop SIL2, and in the unbound IFS structure it is located in the middle of the extended, C-terminal helix α7 (Figure 3). The C-terminal peptide spanning IFS residues 154−161 takes up more than 80% deuterium at long times, one of the highest extents of deuteration in the IFS protein. When bound to SPN, however, the extent of H/DX decreases by 25% at all times. This change is likely due to the repacking of this C-terminal helical segment against the helical core of the IFS protein bound to SPN (Figure 3). These large changes in the kinetics of H/DX for the IFS protein reveal that binding to SPN involves a substantial rearrangement of the C terminus of the IFS structure.

According to the X-ray structure, residues 132−164 form a continuous α-helix (α7) in IFS alone (Figure 3); this region is restructured in the IFS−SPN complex as two α-helices (α7a and α7b) with an intervening loop (residues 139−149 SIL2).[66] The large difference in the extent of H/DX between IFS and the complex for this region raises questions about the true conformation of this segment in solution. The large extents of H/DX for the IFS alone support the conclusion that the conformation of the C-terminal region is dynamic. Moreover, there are large changes in H/DX extents upon binding. The intervening loop, which is closely represented by the peptic peptide 143−151, undergoes considerably less H/DX because it contacts SPN. Additionally, two other peptic peptides, 120−142, containing α7a (128−138), and 154−161, representing most of α7b (150−161), also change considerably in H/DX extents when interacting with SPN. These regions do not, however, directly contact SPN in the crystal structure of the complex

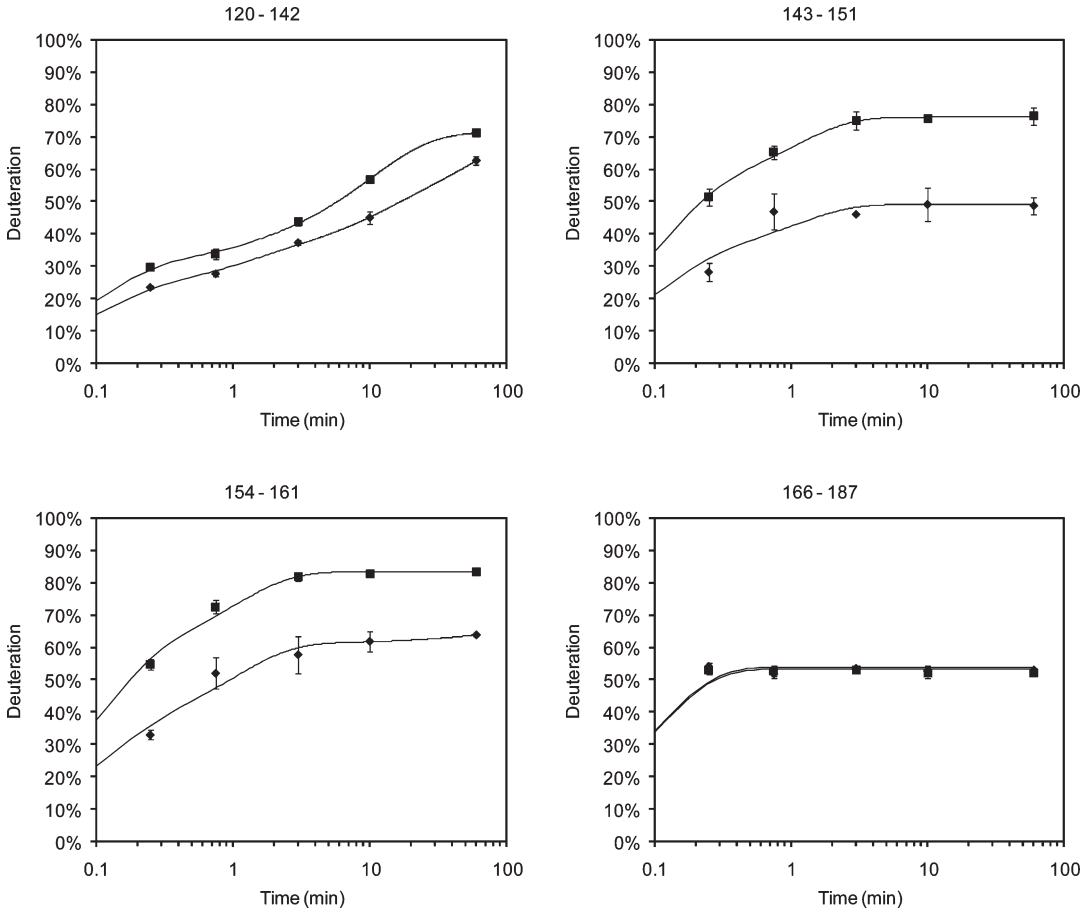

Figure 2. Regions of IFS that show large changes in extents of deuteration upon binding SPN. IFS alone (squares) and 1:1 IFS−SPN complex (diamonds). Residues 166−187 represent the c-Myc and His_6 tags and should not show changes in deuterium incorporation upon binding SPN.

(Figure 3). Instead, they are stabilized by the adjoining interface formation. We conclude that the C-terminal region of IFS alone is less structured in solution than in the crystalline state, whereas for the complex in solution, it adopts a compact folded structure.

Affinity purification tags (c-Myc; EQKLISEEDL, residues 167−176; and His_6, residues 182−187) appended to the C-terminal region of the recombinant IFS protein showed no change in H/DX in the presence and absence of SPN purification tags. Given that this region is not present in the wild type protein from *S. pyogenes*, we expected no difference between the apo and holo forms, and we point to it as an internal control. The peptic peptide, 166−187, is ∼53% deuterated at all H/DX times, whether SPN is present or not (Figure 2).

The N-terminal region of IFS is represented by several peptides from the peptic digest that show no changes in their extents of deuteration upon bonding SPN (Supporting Information, section 1). These peptides span residues 1−14, 15−34, 56−62, 88−91, and 106−119 and are located in the α-helical core of the IFS protein. The N-terminus of IFS^{1-14} shows a constant and high percent deuteration in the absence and presence of SPN. Region 56−62, on the other hand, undergoes modest and nearly constant deuteration in both states, consistent with its location in the hydrophobic core of IFS.

We are unable to draw conclusions for certain regions of IFS because the extents of H/DX could not be measured accurately for the two binding states. The gaps in sequence coverage are for regions 35−55, 63−87, 92−105, 152−153, and 162−165. The peptide 35−55, for example, could be readily identified in H/DX experiments for IFS alone (by both accurate mass and its product-ion spectrum), but the signal-to-noise ratio for peptide detection in the IFS−SPN complex was insufficient to determine accurately the deuterium uptake. Overlapping signals from other peptides eluting at the same time further interfered with detection.

Region-Specific H/D Exchange of SPN. Four peptides derived from the SPN protein show significant changes in H/DX upon binding IFS (Figure 4). A region of SPN represented by residues 282−300 shows the largest changes. In the absence of IFS, the corresponding peptide is >70% deuterated, indicating that it is solvent-exposed or unstructured. In the presence of IFS, the extent of H/DX decreases by 70% at early time points and by 50% at later times. This region comprises one side of SPN's active site cleft and is buried in the IFS−SPN complex, becoming inaccessible for H/DX. No other peptide from IFS or SPN shows such a large change upon formation of the protein−protein complex, and this result highlights the power of H/DX and MS to locate accurately buried interfaces in protein complexess.

The three regions of SPN that show smaller extents of protection upon complexation are represented by peptides 196−220, 349−379, and 393−408. SPN residues 196−220 constitute the other side of SPN's active-site cleft, opposite the 282−300 peptide described above, and residues 196−220 are similarly buried upon binding to IFS (Figure 3). The 349−379 segment is deeper in the SPN active site, but residues 368−370 protrude in a loop that contacts the SIL1 loop (SPN interaction loop 1) of IFS

dx.doi.org/10.1021/bi200244k |*Biochemistry* 2011, 50, 4038–4045

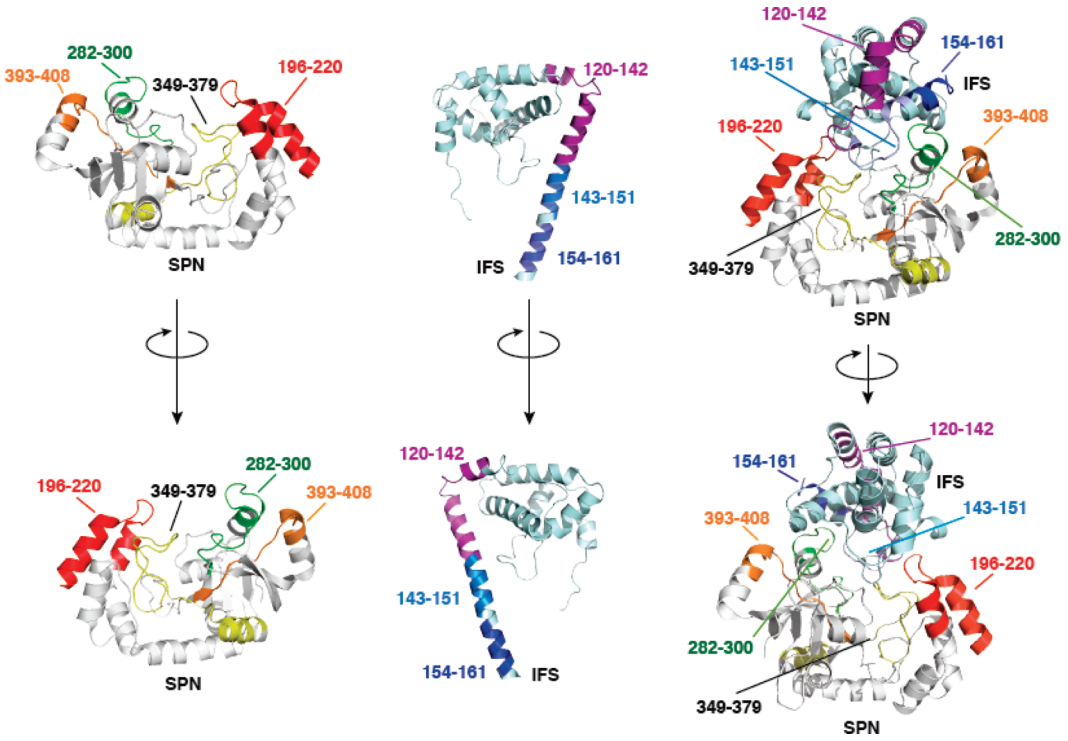

Figure 3. Crystal structure of IFS (PDB entry 3QB2) and the IFS-SPN complex (PDB entry 3PNT), as reported by Smith et al.[66] Several peptides affected by complex formation are highlighted in various colors in both IFS and SPN.

bound to SPN. SPN residues 393−408 form an extended polypeptide that buttresses the 349−379 segment (described above) that is strongly protected in the complex with IFS. Thus, the regions of SPN showing greatest protection upon IFS binding are all located at or around the protein-binding interface that is revealed by X-ray crystallography. Many of these SPN residues are located in connecting loops and turns that protrude from SPN's active site cleft and make direct interactions with the IFS inhibitor. The SPN peptides that are strongly protected from H/DX account for nearly all the residues that directly contact IFS in the crystal structure.

The N-terminal domain of SPN, represented by peptides 80−94, 95−108, 109−141, and 142−172, shows no detectable differences in H/DX upon binding IFS (see Supporting Information, section 2). This region comprises a separate domain required for export of the SPN protein into mammalian cells. It is separated by a proteolytically sensitive linker from the catalytic domain of SPN[64] and was absent from the IFS−SPN complex that was crystallized. Peptide 80−94 is more than 70% deuterated at all H/DX times in both bound and unbound states, indicating that this region is neither highly H-bonded nor involved in the interface. Peptides 95−108 and 109−141 are deuterated to a similar extent compared to the full-length SPN at all H/DX times, whereas peptide 142−172 shows an overall lower extent of deuteration compared to the full-length SPN (35% deuterated in both states after 15 s of H/DX). These results indicate that SPN's N-terminal domain is stably folded, and it does not appear to interact with IFS when it is bound to SPN's catalytic domain.

Two SPN peptides show very low H/DX in both binding states, indicating sites of solvent inaccessibility (Supporting Information, section 2). Peptide 220−234, for example, undergoes 10−15% HDX at 15 s and 40% at 60 min for both states. Region 301−305 undergoes little H/DX (<10%) at all times whether the protein is free or complexed. Both of these peptides are located away from the IFS binding site at the core of the SPN glycohydrolase. Two other peptides (409−417 and 418−451) in the C-terminal region of SPN exhibit little difference in extents of deuteration (<5%) between free and complexed and little protection upon binding to IFS. Correspondingly, they are located distal to the IFS interaction surface. Peptide 313−341 is interesting because it shows no change in response to IFS binding, despite residues Gly330, Val331, and Asp332 participating in interactions with IFS in the crystal structure. The lack of response may simply be that only three residues of 29 are affected.

There are other regions of SPN where we cannot draw conclusions about direct or indirect effects of IFS binding because the extents of deuteration could not be measured accurately for both the free and complexed states. Those regions are represented by peptides 29−79, 173−195, and 235−281. After residue 281, the sequence coverage is nearly 95% for the catalytic domain of SPN.

Summary of Region-Specific H/D Exchange Data. The changes in H/DX reveal those regions of IFS and SPN that become more protected upon complex formation. SPN on the whole decreases its deuteration level by ∼6% upon binding IFS, whereas the smaller IFS protein undergoes ∼12% decrease upon binding to SPN. The regions of SPN most affected by complex formation directly correspond to the binding site for IFS. The IFS subunit, however, undergoes less H/DX in the C-terminal region represented by peptides 120−142 and 154−161, which include a number of residues that do not contact SPN in the crystal structure, and a region represented by 143−151 that does contact SPN. This latter region undergoes a large structural transition between the free and bound conformations of IFS,

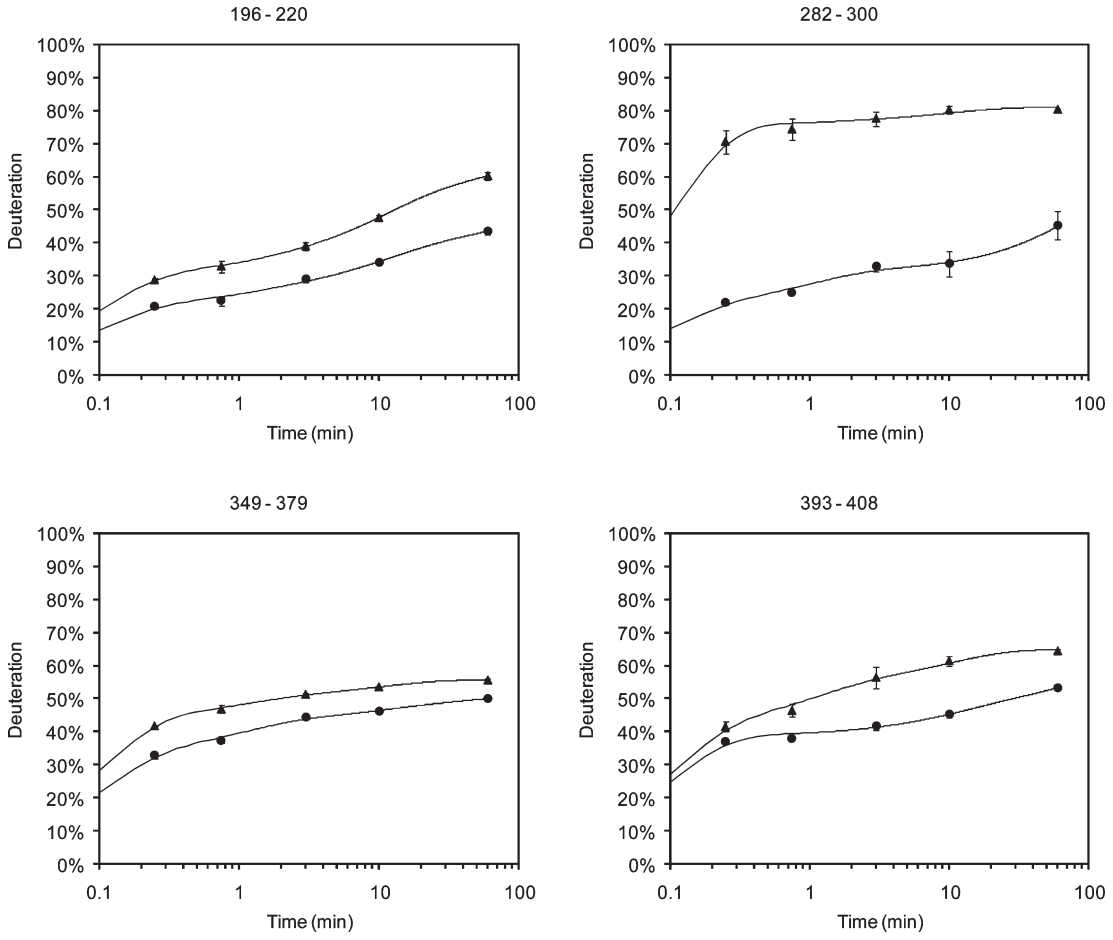

Figure 4. Regions of SPN that show large changes in extents of deuteration upon binding IFS. SPN alone (triangles) and 1:1 IFS−SPN complex (circles).

causing the decreases in the rate of H/DX. The kinetics of H/DX accurately reflects the dynamic interactions of IFS with its cognate toxin, SPN. After 3 min of H/D exchange, a total of 21 additional amide sites are protected in IFS when complexed to SPN as compared to free IFS protein. We can detect eight protected amides in the regions 120−142, 143−151, and 154−161 after 3 min of H/DX, representing 38% of the total change in IFS. Given that we can only account for 38% of the overall change in H/DX, there are other regions not identified that play a role in binding SPN. For example, we were unable to determine changes for peptides from regions 35−55, 63−87, and 92−105 owing to their low signal-to-noise ratios. In contrast, coverage of the SPN catalytic domain is excellent.

FUTURE PROSPECTS

Protein−protein complexes present a challenge in H/DX studies by MS. The number of peptides produced in the pepsin proteolysis of the IFS−SPN complex is greater, of course, than the number from each protein individually. The peptides must be eluted rapidly from the LC column, and overlap in elution can lead to ion suppression. Our inability to monitor certain regions of both proteins results from the insufficient signal-to-noise ratios of coeluting peptides. The use of ultra performance liquid chromatography (UPLC)[71] should ameliorate this problem because it offers increased chromatographic resolution by using a combination of high pressure and small particle sizes in the C_{18} column. Another approach is to complement H/DX with other chemical footprinting experiments including reactions with OH radicals and specific reactions of lysine, for example. These approaches can take advantage of higher resolution liquid chromatography because they make an irreversible covalent change on the proteins.

ASSOCIATED CONTENT

Supporting Information. Several additional examples of region-specific data from IFS and SPN. This material is available free of charge via the Internet at http://pubs.acs.org.

AUTHOR INFORMATION

Corresponding Author

*Tel: (314) 935-4814. Fax: (314) 935-7484. E-mail: mgross@wustl.edu.

Funding Sources

This research was supported by the NCRR of the NIH (Grant No. 2P41RR000954) to M.L.G. and NIGMS (R01GM52504) to T.E.E. This study was also supported in part by UNCF/Merck Science initiative postdoctoral fellowship awarded to C.L.S. and also by an unrestricted grant from Schering Plough (Merck) to M.L.G. (M.L.G. was a consultant for Schering Plough).

■ ACKNOWLEDGMENT

We thank Dr. Henry Rohrs for his assistance with the LTQ-Orbitrap studies and the database searching.

■ ABBREVIATIONS

SPN, *Streptococcus pyogenes* NAD^+ hydrolase; IFS, immunity factor for SPN; MS, mass spectrometry; ESI-MS, electrospray ionization mass spectrometry; Da, dalton; H/DX, hydrogen/deuterium exchange; cryo-EM, cryo-electron microscopy; NMR, nuclear magnetic resonance; IR, infrared microscopy; Y2H, yeast two-hybrid assay; FRET, fluorescence resonance energy transfer; NAD, nicotinamide adenine dinucleotide; D_2O, deuterium oxide; HCl, hydrochloric acid; HPLC, high performance liquid chromatography; UPLC, ultra performance liquid chromatography; Q-TOF, quadrupole time-of-flight; MaxEnt, maximum entropy; SIL, SPN-intervening loop.

■ REFERENCES

(1) Alberts, B. (1998) The cell as a collection of protein machines: preparing the next generation of molecular biologists. *Cell 92*, 291–294.

(2) Aytuna, A. S., Gursoy, A., and Keskin, O. (2005) Prediction of protein-protein interactions by combining structure and sequence conservation in protein interfaces. *Bioinformatics 21*, 2850–2855.

(3) Nariai, N., Kolaczyk, E. D., and Kasif, S. (2007) Probabilistic protein function prediction from heterogeneous genome-wide data. *PLoS One 2*, e337.

(4) Punta, M., Forrest, L. R., Bigelow, H., Kernytsky, A., Liu, J., and Rost, B. (2007) Membrane protein prediction methods. *Methods 41*, 460–474.

(5) Sharan, R., Ulitsky, I., and Shamir, R. (2007) Network-based prediction of protein function. *Mol. Syst. Biol. 3*, 1–13.

(6) Bahadur, R. P., and Zacharias, M. (2008) The interface of protein-protein complexes: analysis of contacts and prediction of interactions. *Cell. Mol. Life Sci. 65*, 1059–1072.

(7) Chothia, C., and Janin, J. (1975) Principles of protein-protein recognition. *Nature 256*, 705–708.

(8) Keskin, O., Gursoy, A., Ma, B., and Nussinov, R. (2008) Principles of protein-protein interactions: what are the preferred ways for proteins to interact? *Chem. Rev. 108*, 1225–1244.

(9) Yan, C., Wu, F., Jernigan, R. L., Dobbs, D., and Honavar, V. (2008) Characterization of protein-protein interfaces. *Protein J. 27*, 59–70.

(10) Janin, J. (1995) Principles of protein-protein recognition from structure to thermodynamics. *Biochimie 77*, 497–505.

(11) Kleanthous, C. (2000) *Protein-Protein Recognition*, Oxford University Press, Oxford, NY.

(12) Spolar, R. S., Ha, J. H., and Record, M. T. (1989) Hydrophobic effect in protein folding and other noncovalent processes involving proteins. *Proc. Natl. Acad. Sci. U.S.A. 86*, 8382–8385.

(13) Young, L., Jernigan, R. L., and Covell, D. G. (1994) A role for surface hydrophobicity in protein-protein recognition. *Protein Sci. 3*, 717–729.

(14) Tsai, C.-J., Lin, S. L., Wolfson, H. J., and Nussinov, R. (1997) Studies of protein-protein interfaces: a statistical analysis of the hydrophobic effect. *Protein Sci. 6*, 53–64.

(15) Xu, D., Lin, S. L., and Nussinov, R. (1997) Protein binding versus protein folding: the role of hydrophylic bridges in protein associations. *J. Mol. Biol. 265*, 68–84.

(16) Norel, R., Sheinerman, F., Petrey, D., and Honig, B. (2001) Electrostatic contributions to protein-protein interactions: fast energetic filters for docking and their physical basis. *Protein Sci. 10*, 2147–2161.

(17) Sheinerman, F. B., Norel, R., and Honig, B. (2000) Electrostatic aspects of protein-protein interactions. *Curr. Opin. Struct. Biol. 10*, 153–159.

(18) Jeffrey, G. A., Saenger, W. (1991) *Hydrogen Bonding in Biological Structures*, Springer-Verlag, Berlin.

(19) Jiang, L., and Lai, L. (2002) CH---O Hydrogen bonds at protein-protein interfaces. *J. Biol. Chem. 277*, 37732–37740.

(20) Baker, E. N., and Hubbard, R. E. (1984) Hydrogen bonding in globular proteins. *Prog. Biophys. Mol. Biol. 44*, 97–179.

(21) Chiu, W., McGough, A., Sherman, M., and Schmid, M. F. (1999) High-resolution electron cryomicroscopy of macromolecular assemblies. *Trends Cell Biol. 9*, 154–159.

(22) Yi, Q., Erman, J. E., and Satterlee, J. D. (1994) Studies of protein-protein association between yeast cytochrome *c* peroxidase and yeast iso-1 ferricytochrome *c* by hydrogen-deuterium exchange labeling and proton NMR spectroscopy. *Biochemistry 33*, 12032–12041.

(23) Fiaux, J., Bertelsen, E. B., Horwich, A. L., and Wuthrich, K. (2002) NMR analysis of a 900K GroEL GroES complex. *Nature 418*, 207–211.

(24) Takahashi, H., Nakanishi, T., Kami, K., Arata, Y., and Shimada, I. (2000) A novel NMR method for determining the interfaces of large protein-protein complexes. *Nat. Struct. Biol. 7*, 220–223.

(25) Zuiderweg, E. R. (2002) Mapping protein-protein interactions in solution by NMR spectroscopy. *Biochemistry 41*, 1–7.

(26) Li, T. (2004) Investigation of protein-protein interactions by isotope-edited Fourier transformed infrared spectroscopy. *Spectroscopy 18*, 397–406.

(27) Fields, S., and Song, O. (1989) A novel genetic system to detect protein-protein interactions. *Nature 340*, 245–246.

(28) Stansfield, I., Stark, M. J. R. (2007) *Yeast Gene Analysis*, pp 139−164, Academic Press, New York.

(29) Truong, K., and Ikura, M. (2001) The use of FRET imaging microscopy to detect protein-protein interactions and protein conformational changes *in vivo*. *Curr. Opin. Struct. Biol. 11*, 573–578.

(30) Yan, Y., and Marriott, G. (2003) Analysis of protein interactions using fluorescence technologies. *Curr. Opin. Struct. Biol. 7*, 635–640.

(31) Yusupov, M. M., Yusupova, G. Z., Baucom, A., Lieberman, K., Earnest, T. N., Cate, J. H., and Noller, H. F. (2001) Crystal structure of the ribosome at 5.5 A resolution. *Science 292*, 883–896.

(32) Braig, K., Otwinowski, Z., Hegde, R., Boisvert, D. C., Joachimiak, A., Horwich, A. L., and Sigler, P. B. (1994) The crystal structure of the bacterial chaperonin GroEL at 2.8 A. *Nature 371*, 578–586.

(33) Williams, S. P., Kuyper, L. F., and Pearce, K. H. (2005) Recent applications of protein crystallography and structure-guided drug design. *Curr. Opin. Chem. Biol. 9*, 371–380.

(34) Russel, R. B., Alber, F., Aloy, P., Davis, F. P., Korkin, D., Pichaud, M., Topf, M., and Sali, A. (2004) A structural perspective on protein-protein interactions. *Curr. Opin. Struct. Biol. 14*, 313–324.

(35) Gingras, A.-C., Gstaiger, M., Raught, B., and Aebersold, R. (2007) Analysis of protein complexes using mass spectrometry. *Nat. Rev. Mol. Cell Biol. 8*, 645–654.

(36) Zhou, M., and Robinson, C. V. (2010) When proteomics meets structural biology. *Trends Biochem. Sci. 35*, 522–529.

(37) Gavin, A.-C., Maeda, K., and Kühner, S. (2011) Recent advances in charting protein-protein interaction: mass spectrometry-based approaches. *Curr. Opin. Biotechnol. 22*, 42–49.

(38) Kaltashov, I. A., Bobst, C. E., and Abzalimov, R. R. (2009) H/D Exchange and Mass Spectrometry in the Studies of Protein Conformation and Dynamics: Is There a Need for a Top-Down Approach? *Anal. Chem. 81*, 7892–7899.

(39) Suchanova, B., and Tuma, R. (2008) Folding and assembly of large macromolecular complexes monitored by hydrogen-deuterium exchange and mass spectrometry. *Microb. Cell Fact. 7*, 12.

(40) Konermann, L., Stocks, B. B., Pan, Y., and Tong, X. (2010) Mass spectrometry combined with oxidative labeling for exploring protein structure and folding. *Mass Spectrom. Rev. 29*, 651–667.

(41) Fitzgerald, M. C., and West, G. M. (2009) Painting Proteins with Covalent Labels: What's in the Picture? *J. Am. Soc. Mass Spectrom. 20*, 1193–1206.

(42) Sinz, A. (2010) Investigation of protein-protein interactions in living cells by chemical crosslinking and mass spectrometry. *Anal. Bioanal. Chem. 397*, 3433–3440.

(43) Low, D. H. P., Frecer, V., Saux, A. L., Srinivasan, G. A., Ho, B., Chen, J., and Ding, J. L. (2010) Molecular Interfaces of the Galactose-binding Protein Tectonin Domains in Host-Pathogen Interaction. *J. Biol. Chem. 285*, 9898–9907.

(44) Mendillo, M. L., Hargreaves, V. V., Jamison, J. W., Mo, A. O., Li, S., Putnam, C. D., Woods, V. L., Jr., and Kolodner, R. D. (2009) A conserved MutS homolog connector domain interface interacts with MutL homologs. *Proc. Natl. Acad. Sci. 106*, 22223–22228.

(45) Hamuro, Y., Coales, S. J., Hamuro, L. L., Woods, V. L., Jr. (2008) Use of enhanced peptide amide hydrogen/deuterium exchange-mass spectrometry (DXMS) in the examination of protein-protein interactions in *Mass Spectrometry Analysis for Protein-Protein Interactions and Dynamics* (Chance, M. R., Ed.), pp 123−155, John Wiley & Sons, Inc., Noboken, NJ.

(46) Komives, E. A. (2008) Deuterium exchange approaches for examining protein interactions: case studies of complex formation in *Mass Spectrometry Analysis for Protein-Protein Interactions and Dynamics* (Chance, M. R., Ed.), John Wiley & Sons, Inc., Hoboken, NJ.

(47) Mitchell, J. L., Engen, J. R. (2009) *Protein Analysis with Hydrogen-Deuterium Exchange Mass Spectrometry*, Elsevier B.V., Amsterdam, The Netherlands.

(48) Zhang, H.-M., Kazazic, S., Schaub, T. M., Tipton, J. D., Emmett, M. R., and Marshall, A. G. (2008) Enhanced Digestion Efficiency, Peptide Ionization Efficiency, and Sequence Resolution for Protein Hydrogen/Deuterium Exchange Monitored by Fourier Transform Ion Cyclotron Resonance Mass Spectrometry. *Anal. Chem. 80*, 9034–9041.

(49) Bennett, M. J., Chik, J. K., Slysz, G. W., Luchko, T., Tuszynski, J., Sackett, D. L., and Schriemer, D. C. (2009) Structural Mass Spectrometry of the .alpha.beta.-Tubulin Dimer Supports a Revised Model of Microtubule Assembly. *Biochemistry 48*, 4858–4870.

(50) Bhavsar, A. P., Guttman, J. A., and Finlay, B. B. (2007) Manipulation of host-cell pathways by bacterial pathogens. *Nature 449*, 827–834.

(51) Cash, P. (2008) Proteomics of bacterial pathogens. *Expert Opin. Drug Discovery 3*, 461–473.

(52) Pichichero, M. E., and Casey, J. R. (2007) Systematic review of factors contributing to penicillin treatment failure in *Streptococcus pyogenes* pharyngitis. *Otolaryngol.—Head Neck Surg. 137*, 851–857.

(53) Stollerman, G. H., and Dale, J. B. (2008) The importance of the Group A *Streptococcus* capsule in the pathogenesis of human infections: a historical perspective. *Clin. Infect. Dis. 46*, 1038–1045.

(54) Stevens, D. L., Salmi, D. B., McIndoo, E. R., and Bryant, A. E. (2000) Molecular epidemiology of nga and NAD glycohydrolase/ADP-ribosyltransferase activity among *Streptococcus pyogenes* causing streptococcal toxic shock syndrome. *J. Infect. Dis. 182*, 1117–1128.

(55) Cunningham, M. W. (2000) Pathogenesis of group A streptococcal infections. *Clin. Microbiol. Rev. 13*, 470–511.

(56) Bricker, A. L., Carey, V. J., and Wessels, M. R. (2005) Role of NADase in virulence in experimental invasive group A streptococcal infection. *Infect. Immun. 73*, 6562–6566.

(57) Meehl, M. A., Pinkner, J. S., Anderson, P. J., Hultgren, S. J., and Caparon, M. G. (2005) A novel endogenous inhibitor of the secreted streptococcal NAD-glycohydrolase. *PLoS Pathogens 1*, 0362–0372.

(58) Bernheimer, A. W., Lazarides, P. D., and Wilson, A. T. (1957) Diphosphopyridine nucleotidase as an extracellular product of streptococcal growth and its possible relationsip to leukotoxicity. *J. Exp. Med. 106*, 27–37.

(59) Carlson, A. S., Kellner, A., Bernheimer, A. W., and Freeman, E. B. (1957) A stretococcal enzyme that acts specifically upon diphosphopyridine nuleotide: characterization of the enzyme and its separation from streptolysin O. *J. Exp. Med. 106*, 15–26.

(60) Gerlach, D., Ozegowski, J. H., Gunther, E., Vettermann, S., and Kohler, W. (1996) Purification and some properties of streptococcal NAD-glycohydrolase. *FEMS Microbiol. Lett. 136*, 71–78.

(61) Karasawa, T., Takasawa, S., Yamakawa, K., Yonekura, H., Okamoto, H., and Nakamura, S. (1995) NAD(+)-glycohydrolase from *Streptococcus pyogenes* shows cyclic ADP-ribose forming activity. *FEMS Microbiol. Lett. 130*, 201–204.

(62) Kimoto, H., Fujii, Y., Hirano, S., Yokota, Y., and Taketo, A. (2006) Genetic and biochemical protperties of streptococcal NAD-glycohydrolase inhibitor. *J. Biol. Chem. 281*, 9181–9189.

(63) Ghosh, J., Anderson, P. J., Chandrasekaran, S., and Caparon, M. G. (2010) Characterization of Streptococcus pyogenes beta-NAD+ glycohydrolase: re-evaluation of enzymatic properties associated with pathogenesis. *J. Biol. Chem. 285*, 5683–5694.

(64) Ghosh, J., and Caparon, M. G. (2006) Specificity of *Streptococcus pyogenes* NAD^+ glycohydrolase in cytolysin-mediated translocation. *Mol. Microbiol. 62*, 1203–1214.

(65) Tatsuno, I., Sawai, J., Okamoto, A., Matsumoto, M., Minami, M., Isaka, M., Ohta, M., and Hasegawa, T. (2007) Characterization of the NAD-glycohydrolase in streptococcal strains. *Microbiology 153*, 4253–4260.

(66) Smith, C. L., Ghosh, J., Elam, J. S., Pinkner, J. S., Hultgren, S. J., Caparon, M. G., and Ellenberger, T. (2011) Structural Basis of *Streptococcus pyogenes* Immunity to Its NAD^+ Glycohydrolase Toxin. *Structure 19*, 192–202.

(67) Spolar, R. S., and Record, M. T. (1994) Coupling of local folding to site-specific binding of proteins to DNA. *Science 263*, 777–784.

(68) Wright, P. E., and Dyson, H. J. (2009) Linking folding and binding. *Curr. Opin. Struct. Biol. 19*, 31–38.

(69) Weis, D. D., Engen, J. R., and Kass, I. J. (2006) Semi-automated data processing of hydrogen exchange mass spectra using *HX-Express*. *J. Am. Soc. Mass Spectrom. 17*, 1700–1703.

(70) Sperry, J. B., Shi, X., Rempel, D. L., Nishimura, Y., Akashi, S., and Gross, M. L. (2008) A Mass Spectrometric Approach to the Study of DNA-Binding Proteins: Interaction of Human TRF2 with Telomeric DNA. *Biochemistry 47*, 1797–1807.

(71) Wales, T. E., Fadgen, K. E., Gerhardt, G. C., and Engen, J. R. (2008) High-Speed and High-Resolution UPLC Separation at Zero Degrees Celsius. *Anal. Chem. 80*, 6815–6820.